Rheol Acta 36:591–609 (1997)

ORIGINAL CONTRIBUTION

Physical gelation under shear for gelatin gels

Walter de Carvalho
Madeleine Djabourov

Received: 24 June 1997
Accepted: 9 September 1997

W. de Carvalho · M. Djabourov (✉)
Laboratoire de Physique et Mécanique des Milieux Hétérogènes
CNRS URA 857
ESPCI
10 Rue Vauquelin
Paris, Cedex 05 75231, France

Abstract Physical gelation is the process of crosslinking which reversibly transforms a solution of polymers into a gel. The crosslinks of the network have a physical origin (hydrogen bonding, Van der Waals forces...) and therefore are sensitive to variations of temperature, pH, ionic content, etc. (non-permanent crosslinks). Physical and chemical gelation have been extensively studied in quiescent conditions, where rheology experiments have been performed to follow the network formation without disturbing the process. In this study we consider gelation of a well known physical, thermoreversible, gel (gelatin gel), which proceeds under flowing conditions. The gelling solution is submitted to a shearing, with imposed, permanent shear stresses or imposed, permanent, shear rates. Under flow, a competition arises between the formation of clusters by physical crosslinking and their disruption by the shear forces. This investigation defines the flowing conditions which either allow or impede gel formation. In particular, a critical shear rate $\dot{\gamma}*$, related to the gelation temperature and gelatin concentration, is identified which separates the two regimes. A microscopic model is proposed, based on the analysis of flow curves and dynamic measurements, which describes the structure of the gelling solution: microgel particles grow to a maximum size which depends on the flow. When the volume fraction of particles is high enough, percolation between particles occurs suddenly and a yield stress fluid is formed (particulate gel). The differences between gels made in quiescent conditions and gels made under flow are underlined.

Key words Physical gelation – sheared gels – microgels – gelatin – gel processing

Introduction

The influence of shear on phase diagrams of complex fluids has received increasing attention during the last decade, involving theoretical analysis, combined experimental approaches and computer simulations (Rangel-Nafaile, 1984; Larson, 1992). Processes in industry, which include stages of mixing, pumping, flowing of complex fluids, involve these situations. A large variety of systems has been considered in the literature, starting with binary liquid mixtures and evolving towards polymer solutions, polymer blends, block copolymers, colloidal suspensions, surfactant solutions, emulsions, etc. The experimental effort was focused on developing new facilities which allow structural measurements simultaneously to the flow such as optical spectroscopy (birefringence, fluorescence, dichroism), scattering techniques (light, x-ray or small-angle neutron) or microscopic observations under flow. Computer simultations dealt with aggregation of a large number of particles. Both shear-induced aggregation of an initially dispersed

RA 860

Rheologica Acta, Vol. 36, No. 6 (1997)

configuration (Doi and Chen, 1989) and rupturing of fully aggregated particulate gels (West et al. 1994) were considered.

A brief survey of the literature is made by referring to the type of material investigated.

– *Binary liquid mixtures* of small molecules near the critical point were first investigated by Beysens et al. (1983) and Chan et al. (1991), following the theoretical work of Onuki and Kawasaki (1979). The authors showed by small-angle light scattering that the critical fluctuations in the one-phase region become anisotropic and that the critical temperature is shifted downward by shear. Min and Goldburg (1993) investigated by dynamic light scattering nucleation in the metastable state of binary mixtures of simple liquids induced by a sudden quenching through the two-phase boundary, in the presence of shear. They observed that shear creates a dynamical equilibrium by rupturing droplets of the minority phase when they have grown to sufficient size. When the shear rate is high enough that the fragments are under the thermodynamic critical size of nucleation, then shear-induced mixing occurs. A steady state droplet narrow distribution is observed, determined by the supercooling and the shear rate.

– Model calculations dealing with the thermodynamics of phase separation of sheared polymer solutions and blends have been extensively examined by Wolf since 1984 (Wolf, 1984; Horst and Wolf, 1993). Phase separations in *synthetic polymer solutions* under shear have also been observed by Hashimoto et al. (1988) for a polymer mixture (polystyrene and polybutadiene with a commonly good solvent) with the aim of highlighting specific features of polymer dynamics, in contrast to the dynamics of binary mixtures of simple fluids. Here the technique used is small-angle light scattering and the solutions were near the critical composition, in the two-phase region. The experimental studies show a complex pattern with several regimes in the shear rate dependence of the concentration fluctuations.

– Binary *polymer blends* under shear have been studied by small-angle neutron scattering techniques by Nakatani et al. (1990). In this case the experiments were focused in the one-phase region, near the critical temperature, for two homopolymer blends of high molecular weight. For low molecular weight polymer blends (deuterated polystyrene and polybutadiene) Hobbie et al. (1992) established that shear inhibits phase separation at the critical molecular composition: the flow starts breaking up the long-range critical fluctuations when the shear rate becomes comparable to the equilibrium relaxation rate of these fluctuations.

– Changes of spatial organizations under shear have been observed in *surfactant solutions* close to the micellar to lamellar phase transition and show that the transition can be induced by shear; the long micelles are first aligned in the direction of the flow, then form compact nematic structures (Decruppe et al., 1994). Other isotropic to nematic transitions in worm-like micelles have been reported by Berret et al. (1994). Successive transitions in lamellar phases under shear were observed with formation of multilayer spherical droplets of well defined sizes (Diat et al., 1993).

– Other examples come from *emulsions* submitted to high shears where emulsification can lead to rupturing of the droplets down to a unique size (Mason and Bibette, 1996).

– The first studies on aggregation of *globular proteins* in solution in presence of shear were conducted in the 1950's with the pioneer work of Joly and Barbu (1949–1950), Joly (1951–1962). Flow birefringence experiments were used in order to follow the denaturation of the proteins and the growth of linear aggregates for different physical-chemical environments. High shear rates were shown to induce fragmentation of the chains. However, Joly noticed that shear can also provoke aggregation of particles in a variety of systems (tobacco mosaic viruses, serum albumin proteins). Then, the solutions become turbid. He named these effects "rheoturbidity" and proposed a theory to explain it (Joly, 1962). Gelatin gelation was also investigated by the same techniques (flow birefringence) by Bourgoin and Joly (1952–1958). Gelatin concentrations were low (<1%) and did not lead to a gel state. The authors tried to determine the size of the clusters of chains without disturbing the process. They noticed that the shear modified the structure of the solutions and they tried to avoid this "source of error" as much as possible in their measurements. Interpretation of the results was based on the notion of "kinetic units" that can be deformed and ruptured by shear.

The consequences of shearing upon gelation for polymer solutions has not been considered so far, from a fundamental point of view. Gelation in quiescent conditions has been analyzed within the same theoretical framework as critical phase transitions (de Gennes and Stauffer, 1976). The parallel between the critical temperature T_c as defined, for instance, at the liquid-vapor critical point of pure liquids and the fraction of reacted bonds at the gel point, p_c, led to a precise and general description of gelation focused especially on the determination of scaling laws in the vicinity of the gel point. In this paper we consider the case of the physical gelation for a polymer solution under shear. Shearing sets a competition between aggregation of the chains into clusters of growing sizes and disruption of the clusters by hydrodynamic forces.

In this paper the gelatin gel is taken as an example. The aim of this work was to put into evidence the ef-

fects of mechanical actions on the process of gelation, keeping the same temperature history as for making the gel in quiescent conditions. Only rheological experiments were performed in this study. To investigate a physical gelation under shear in well controlled conditions we considered two ideal situations: gelation proceeds under flow at imposed shear stresses or at imposed shear rates. The paper is divided into four sections: materials and experimental set-up are introduced first, then the protocols of measurements corresponding to the two types of experiments (stress or shear rate control) are presented. Results and comments are given afterwards, and finally a tentative interpretation of the rheological measurements in terms of structure of the solution is found in the last section. We conclude with an outlook for future experiments.

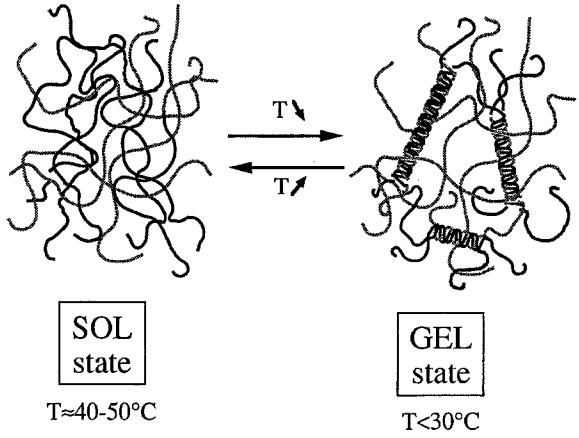

Fig. 1 The coil-helix transition in gelatin gels

Materials and methods

Gelatin gels are typical examples of thermoreversible gels (for a recent review, see te Nijenhuis (1997)). Gelatin is a biopolymer; it is the protein of collagen which has been extracted from bones or from skin and which has lost its native conformation of triple helices assembled into fibers. At rest, a gelatin solution, with a concentration of a few percent in protein, sets when the temperature is lowered below approximately 30 °C; a fluid solution (sol state) is obtained above 40 °C (Djabourov et al., 1988a,b). The sol-gel transition is reversible in temperature with a hysteresis of a few degrees. Gelation is induced by the partial recovery of the native conformation of the chains in triple helices which join several chains together (see Fig. 1). The amount of triple helices depends on temperature and increases as a function of time, at a given temperature.

The sol-gel transition of this system is a kinetic process. As renaturation proceeds, a network is created whose elastic modulus increases with time. The sol-gel transition of gelatin (Djabourov et al., 1988b) was found to obey the general scheme of percolation, and exhibits a gel point which depends only on the amount of renaturated helices (fraction of reacted bonds), independent of the gelation temperature or time needed to reach the gel point. The elastic moduli, in particular, follow the predicted scaling laws.

The gelatin sample used in this study has been kindly provided by Systemes Bio Industries (SBI) and it is a Rousselot-type gelatin extracted from bones with a photographic grade. The molecular weight distribution has been published elsewhere (Djabourov et al., 1988a). Gelatin was first let to swell into demineralized water at 4 °C, then dissolved by heating the solution at 50 °C during 1 h using a magnetic stirrer. Concentrations are given in weight of gelatin/total weight. pH of the solutions were around 5.8. The rheological experiments were performed using a Carrimed CSL 100 instrument, which is a stress-controlled rheometer. We used a cone and plate geometry with a diameter of 4 cm and a cone angle of 2° and a lid preventing water evaporation. Temperature is controlled by a Peltier device. The rheometer has been run either in flow or in oscillation, with shear stress, shear rate or shear strain control. Different types of measurements were linked together.

Protocols for measurements

The protocols for performing gelation under shear were specially adapted to the process of gelation for gelatin gels. Gelation is promoted by lowering the temperature from the dissolution temperature (45 °C) to any temperature below 30 °C. The lower the temperature, the more rapid gelation occurs. When a suitable gelation temperature has been chosen, the process can be followed in time by rheological measurements.

The following temperature and rheological protocols have been adopted (de Carvalho and Djabourov, 1994, 1995):

- the rheometer was initially set to 45 °C, then the solution was poured and let to equilibrate during 1 min, then temperature was lowered to 26 °C in 2 min and left constant during all the remaining time. This quick temperature lowering can be considered as a thermal quench for the solution. Temperature was varied exactly in the same way for the shear stress or shear rate-controlled experiments;
- the rheological protocols are aimed firstly to impose the different shearing conditions to the gelling solution and to follow continuously the changes which occur, then to provide a full characterization of the fluid state at any stage of the process, based on measurements in linear and non-linear regimes.

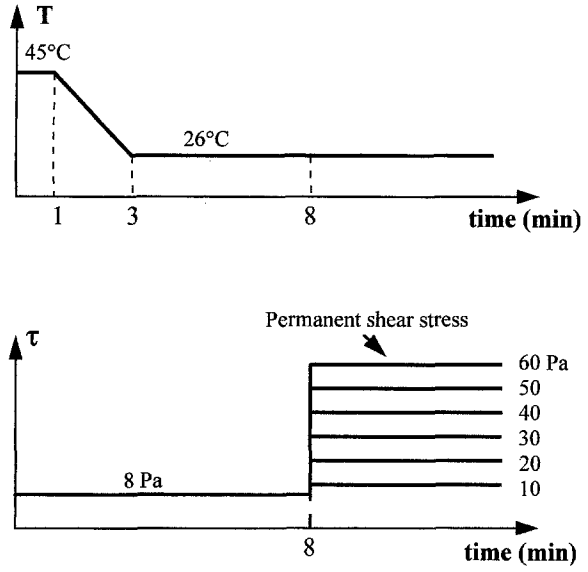

Fig. 2a Protocols for temperature and shear stress variation for studying gelation under imposed shear stresses

a) Gelation under constant, permanently imposed shear stresses

Protocols are shown in Fig. 2a. Starting at time $t=0$, during the first minute, when the solution is at 45 °C, a low shear stress, τ, of 8 Pa was applied, which provides a measurement for the initial viscosity of the solutions. This low stress was kept during the next 7 min, when the solution was cooled to 26 °C. As soon as the temperature was lowered, it was expected that the viscosity starts increasing, and this was indeed observed. After this stage, we decided to apply shear stresses of higher levels which were kept constant during the process. The imposed stresses during gelation varied from 10 to 60 Pa for solutions of concentration 6.5% which were mostly investigated in this study. These shear stresses could not be applied from the very beginning because the rheometer went out of the range of accessible shear rates; letting viscosity increase during a few minutes allows to apply afterwards the desired shear stresses. The shear rates $\dot{\gamma}$ were continuously recorded versus time and an apparent viscosity of the solution η_{app} defined by

$$\eta_{app} = \frac{\tau}{\dot{\gamma}} \qquad (1)$$

was derived. Thus these measurements provide a first insight of the effect of the stress upon the aggregation of the chains in solution. In order to obtain a complete characterization of the state of the solution, we decided to introduce brief interruptions of the applied stress and to submit the solution to various types of shear. The duration of these interruptions was of the order of 1 or 2 min, such as evolution of the viscosity during the

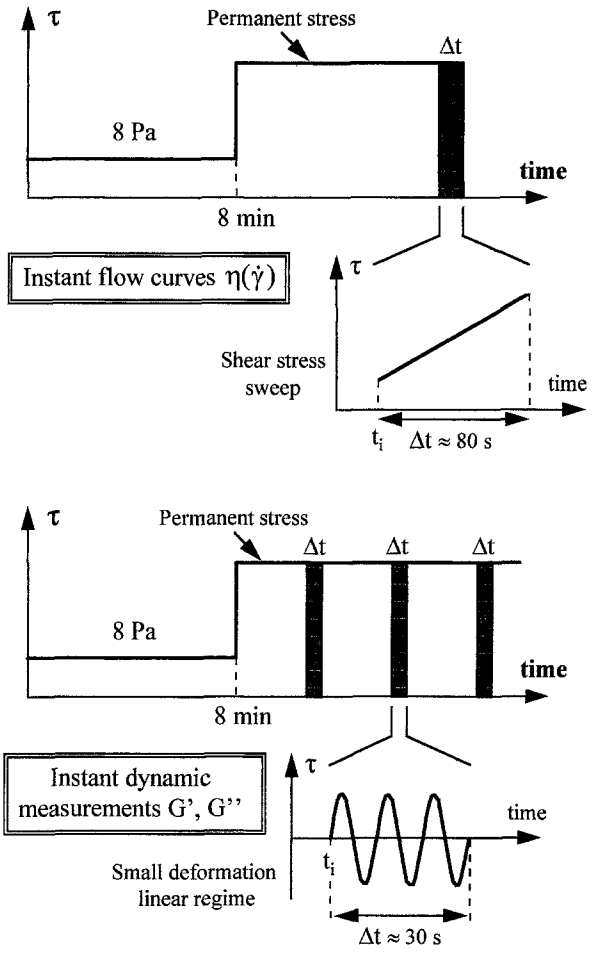

Fig. 2b Instant measurements can be performed by interrupting briefly the imposed stresses and submitting the solution to shear stress sweeps (during $\Delta t = 80$ s) or to small amplitude dynamic measurements ($\Delta t = 30$ s). Instant flow curves $\eta(\dot{\gamma})$ and G', G'' values were derived at times t_i

time should not exceed 10%. During the brief interruptions, we submitted the solution to a sweep of increasing shear stresses, in order to construct the instant rheograms (flow curves) of the solution. Shear stress sweeps must be made slowly enough that the rheograms represent an equilibrium relationship between stress and shear rate. During a kinetic process, the time for performing the sweeps is limited. A compromise had to be found which corresponds to a quasi equilibrium sweep. This point could be checked by performing the step-like increases of the shear stress, instead of a continuous sweep and comparing the two types of rheograms. The results were identical within the experimental error. In some cases, we also performed increasing and decreasing shear sweeps in order to establish whether the rheograms are reversible or not. The sweep started in general below the stress imposed during the flow and ended at larger stresses. We also investigated various ampli-

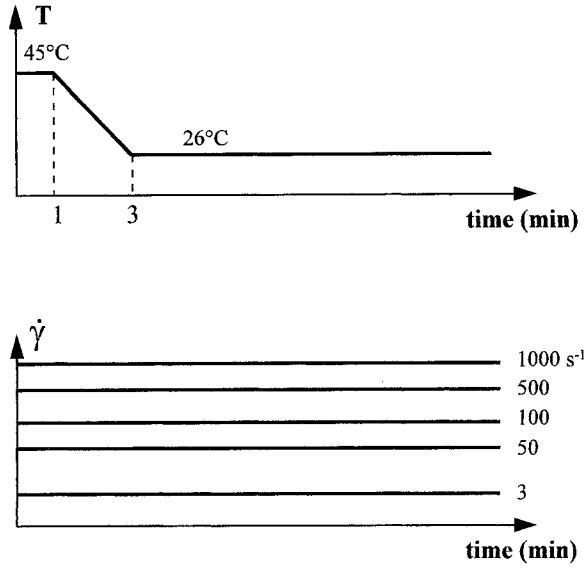

Fig. 3a Protocols for temperature and shear rate variation for studying gelation under imposed shear rates

tudes for the shear sweep. These points will be discussed in the next section. In order to avoid undesired memory effects, a new sample was chosen for each new rheogram. In addition to the shear stress sweeps, we also investigated the dynamic behavior of the solution in the linear range by interrupting briefly the flow during 30 s and performing small amplitude oscillations at frequency of 1 Hz, for deriving G' and G''. These measurements were more easily performed as they are non disturbing and did not require a new sample each time. Instant rheograms and dynamic measurements are schematically represented in Fig. 2b.

b) Gelation under constant, permanently imposed shear rates

The protocols parallel the previous ones, with some minor differences (Fig. 3a, b). The desired shear rate was applied from the beginning, and could be varied from 3 to 1000 s^{-1} with the same geometry. The apparent viscosity was recorded versus time, for the different shear rates. Short interruptions were also introduced in order to explore the state of the fluid. Shear rate sweeps were performed from below to above the flow shear rate. Instant measurements of the dynamic moduli were performed in the linear regime. The protocols for the various instant measurements are summarized in Fig. 3b.

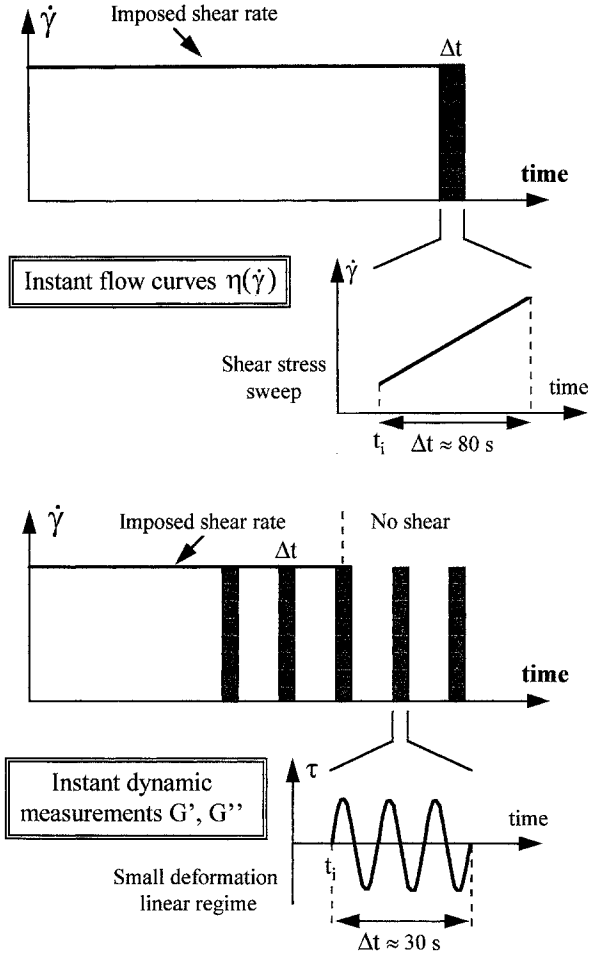

Fig. 3b Instant measurements can be performed by interrupting briefly the imposed rates and submitting the solution to shear rate sweeps (during $\Delta t = 80$ s) or to small amplitude dynamic measurements ($\Delta t = 30$ s). Instant flow curves $\eta(\dot{\gamma})$ and G', G'' values were derived at times t_i

Results

Gelation under fixed shear stresses

A solution with a gelatin concentration is 6.5% sets normally at $T=26\,°C$ within approximately 15 min. The gelatin sample is considered as a quickly gelling one, with a high elastic modulus (Bloom of 256). We report first on the results of *gelation under constant shear stress*. One can see in Fig. 4a the time evolution of the shear rate for different applied shear stresses over 300 min. The shear rate is represented in a logarithmic scale over six decades which is the maximum accessible range for this instrument. The shear rate decreases, which indicates that the solution is thickening. The time evolution of the shear rate, however, depends strongly on the applied shear stress. The stress delays the normal evolution of the solution. The apparent viscosities

Rheologica Acta, Vol. 36, No. 6 (1997)

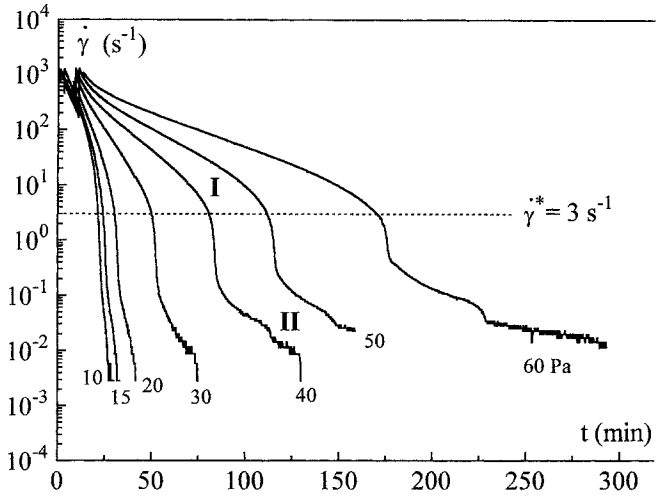

Fig. 4a Kinetics of gelation under constant shear stresses, between 10 and 60 Pa. The shear rate was continuously recorded versus time. Stages I and II and the critical shear rate $\dot{\gamma}^*$ are indicated on the figure. (Gelatin concentration $c = 6.5\%$, $T = 26\,^{\circ}C$)

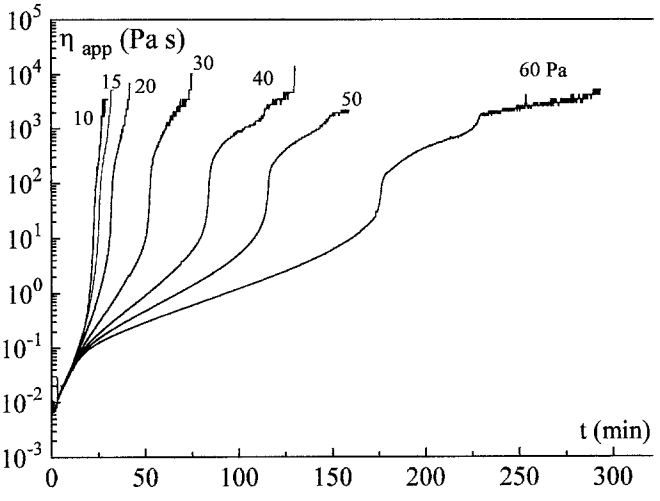

Fig. 4b The apparent viscosities corresponding to the measurements of Fig. 4a

(Eq. (1) for the respective shear stresses are represented in Fig. 4b. In the sol state, the solution is Newtonian with a viscosity of 6.4 mPa s. During the first 15 min the viscosity increases independently of the stress. All the data are superposed, meaning that the solution is Newtonian when gelation starts. The time dependence of the shear rate can be decomposed in two stages (Fig. 4a): in Stage I, a steady decrease of the shear rate is observed, then a sudden decrease appears of one or two orders of magnitude within a few minutes, then again the shear rate decreases during Stage II, more irregularly. The sudden decrease will be called the transition in the following. The transition occurs at various lapses of time t_{tr} from 20 min to 180 min depending on the applied stress. In Fig. 4a it can be seen that the transition begins always when the flow reaches a particular shear rate, independent of the stress. We call this shear rate the critical shear rate $\dot{\gamma}^*$. It is equal to $\dot{\gamma}^* = 3 \pm 1\ s^{-1}$ in Fig. 4a. It will be shown later (in the next section) that the critical shear rate depends only on the gelatin concentration and the gelation temperature. Some time after t_{tr}, rotation of the cone stops, either suddenly (like for 50 or 60 Pa), or when the minimum measurable angular rotation is reached ($1.4\ 10^{-3}\ s^{-1}$) like for 10 to 20 Pa. The end of the process is not completely reproducible. However, in all cases rotation of the cone ceases, indicating that the stress is not high enough to maintain the solution under flow.

One can draw as a first conclusion from these experiments that the stress influences significantly the time dependence of the polymer chain association. The solution, however, reaches a very viscous state ($\eta_{app} = 10^4$ Pa s). A particular shear rate $\dot{\gamma}^*$ plays the role of initiating the transition towards the very viscous state. The nature of this transition will be elucidated in the next experiments.

Instant flow curves (rheograms)

Instant rheograms provide the complementary information on the course of the process. Gelation under a stress $\tau = 40$ Pa is analyzed in detail, but similar results were obtained for stresses of 30 and 60 Pa. The results can be displayed in several ways, each one enlightening a different property. Three different types of plots are shown in Fig. 5. Apparent viscosities versus shear rates, in log-log scales, are given in Fig. 5a, shear stresses versus shear rates, in log-log scales, in Fig. 5b and apparent viscosities versus shear stresses, in log-log scales, in Fig. 5c. The different instants of the measurements are shown in minutes on the curves.

In Fig. 5a, one can see that, during Stage I, the first 84 min, the fluid is shear thinning, characterized by a high viscosity at low shear rates, called the steady shear viscosity. As gelation proceeds, the steady state viscosity increases of three orders of magnitude and the shear thinning domain becomes broader and broader. It is clearly seen that the beginning of the shear thinning domain, at low frequencies, is shifted progressively to lower shear rates with time. A Newtonian limit is expected for infinitely high shear rates, but it is not reached within the accessible range for this geometry (maximum $1.2\ 10^3\ s^{-1}$). The slope in the shear thinning domain of the viscosity increases as gelation proceeds. This indicates a power law behavior of the viscosity versus the shear rate whose exponent increases with time. In Stage II, the viscosity versus shear rate is more difficult to analyze without the help of a model.

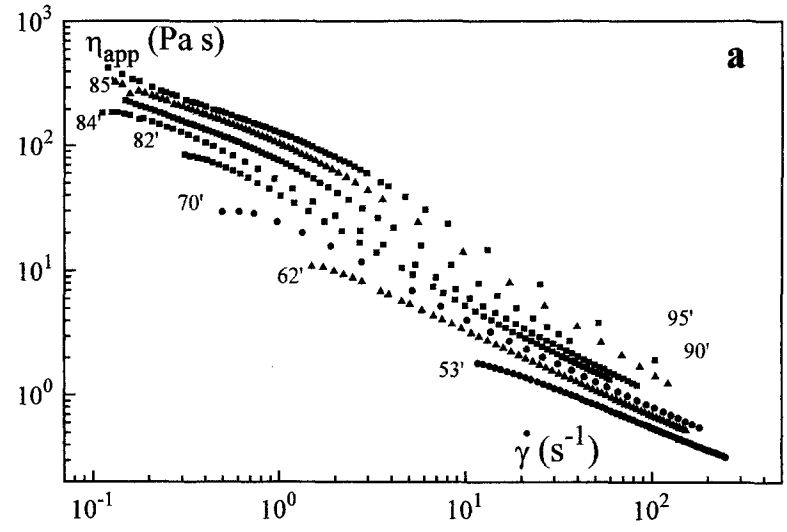

Fig. 5 Instant flow curves (rheograms) for gelation under an imposed shear stress of 40 Pa. The instants are indicated in minutes on the plots. ($c = 6.5\%$, $T = 26\,°C$)

Fig. 5 a Apparent viscosities η_{app} versus shear rates $\dot{\gamma}$, both in logarithmic scales

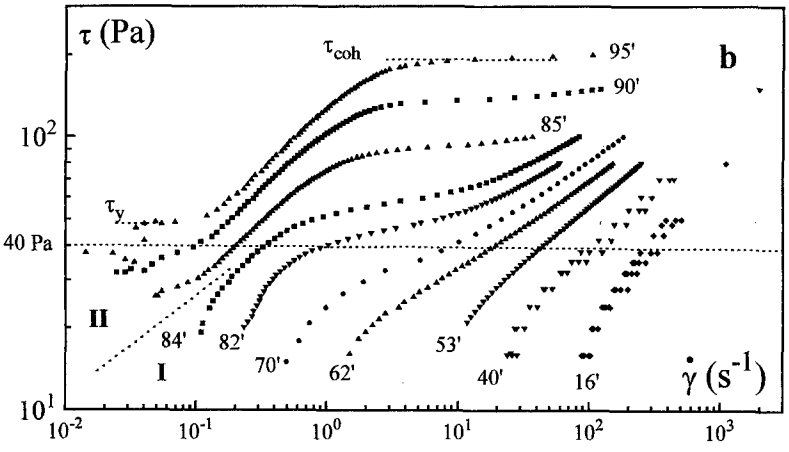

Fig. 5 b Shear stresses, τ, versus shear rates, $\dot{\gamma}$, both in logarithmic scales

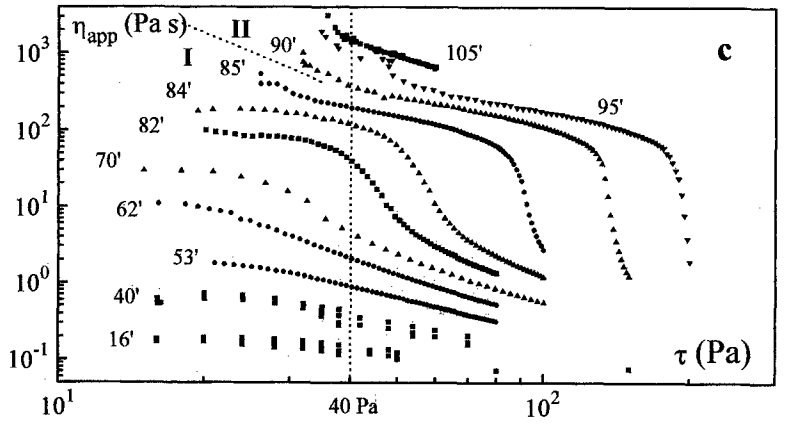

Fig. 5 c Apparent viscosities η_{app} versus shear stresses τ in logarithmic scales

In Fig. 5 b, the log τ versus the log $\dot{\gamma}$ provides a different insight of the rheological state of the fluid. The stress applied continuously during the process is indicated on the plot (τ=40 Pa). One can see that the range of shear stresses, used for all the flow curves in Stage I, is comprised between 20 and 100 Pa, and that the corresponding shear rates decrease, as the solution becomes more and more viscous (Fig. 5 a). Changes of the slope of log τ versus log $\dot{\gamma}$ become very pronounced when approaching the transition time t_{tr}. In particular, at

Rheologica Acta, Vol. 36, No. 6 (1997)

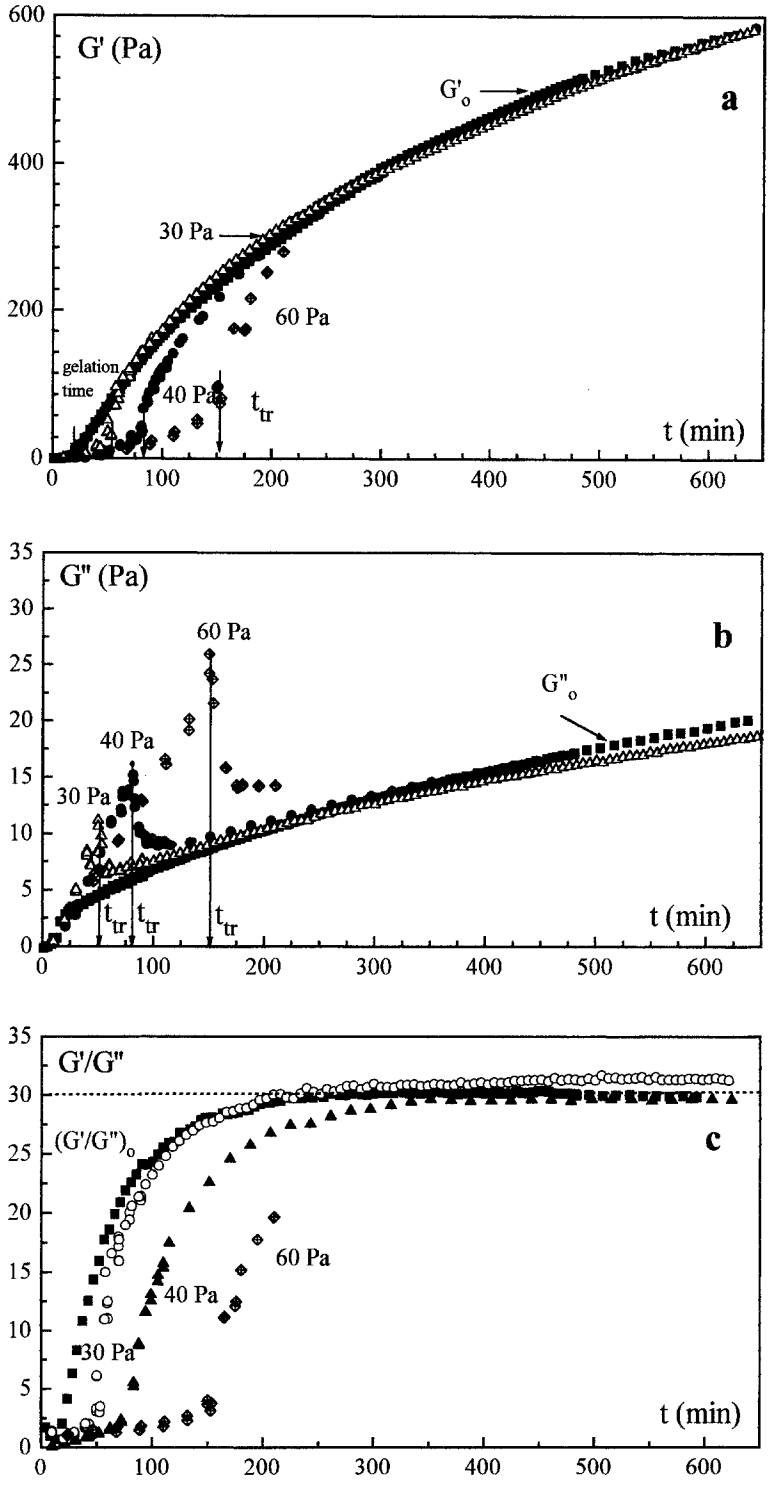

Fig. 6 Dynamic measurements at a frequency of 1 Hz, for gels made in quiescent conditions and under flows at constant shear stresses. The transition times t_{tr} are indicated on the plots. **a** G' versus time, **b** G'' versus time, **c** the ratio G'/G''

$t=84$ min, the rheogram takes a flat shape which indicates that, for a small variation of the stress, in the intermediate range (50 Pa), a very large change of the shear rate appears. This corresponds to a slope of $\log \eta$ versus $\log \dot{\gamma}$ close to -1 (Fig. 5a). The flow for this particular shear stress becomes unstable: if the rheogram was absolutely flat, the shear rate would not be defined for this particular shear stress (unstable flow). This shape of the rheogram announces the transition towards Stage II. In Stage II, the rheograms present two plateau values: one

can see the appearance of a yield stress τ_Y at low shear rates and a second plateau at larger values of the stress. For instance at $t=85$ min the yield stress is $\tau_Y \approx 20$ Pa. The solution became after transition a yield stress fluid. The yield stress is below the applied stress during the process (40 Pa), so that the solution can flow. The yield stress increases with time, reaches the applied stress and the flow stops (end of the continuous plot). After the transition, when the yield stress is very close to the applied stress, the flow is however irregular and "sticky" and can stop at any moment. The second plateau value of the rheograms is called the cohesion stress, τ_{coh}. For instance, at $t=85$ min, $\tau_{coh} = 80$ Pa. When the cohesion stress is reached, the shear rate increases suddenly from a few s^{-1} to more than 100 s^{-1}. Like the yield stress, the cohesion stress increases versus time; however, one can notice that the unstable flows begin close to $\dot{\gamma} = 2$ or 3 s^{-1}. This point will be taken up in the discussion (next section).

In Fig. 5c the apparent viscosity η_{app} is plotted versus the shear stress τ. The strong shear thinning is well evidenced in the end of Stage I and in Stage II, for increasing shear stresses. In Stage II an infinite viscosity appears below the yield stress τ_Y.

Comparsion with gels made at rest: linear properties

Dynamic measurements in the linear range were performed for gels made under flow and compared to gels at rest. The measurements are performed at 1 Hz, during periods of 15 to 20 s, every 10 to 15 min. The transition times for the gelation under shear are indicated. In Fig. 6a, the elastic moduli are shown, in Fig. 6b the loss moduli and in Fig. 6c the ratio G'/G''.

- Figure 6a shows that the elastic modulus of the gel made in quiescent conditions G'_0 starts to increase strongly after about 15 min. (A more detailed investigation has been done at different frequencies, but is not useful for our purpose here). The data for gels made under 30, 40 and 60 Pa are also shown. The elastic moduli increase rapidly after the transition time t_{tr} and tend to reach the values for gels made at rest. The data in Fig. 6a has been also taken after the cone rotation had stopped and shows no discontinuity with the previous measurements.
- Figure 6b, G'' is plotted versus time for gels made at rest, G''_0, or under shear. One can see that the loss moduli for the gels made under shear, before transition, are above the values for the gel made at rest, corresponding to a more viscous than elastic solution. As soon as the transition occurred, the loss moduli decreased towards the values measured at rest.
- Figure 6c summarizes the results of Fig. 6a and b. As a first approximation, one can see that the ratio G'/G'' is similar for gels made under shear and at rest. A slightly larger ratio appears for the gel made under 30 Pa, but the difference might be in the range of reproducibility of the measurements.

Comparison with gels made at rest: non-linear properties

When a gel is made in quiescent conditions and shear stress sweeps are applied at various instants, it can be seen in Fig. 7 that the shapes of the instant rheograms are substantially different from those obtained during gelation under permanent stress. After 15 min an elastic modulus had appeared and the rheograms indicate a plateau value, which can be considered as the cohesion stress of the gel. No yield stress appears. The gel made at rest cannot flow, it breaks under a large enough stress. The cohesion stress increases rapidly in time. We have summarized the results concerning the cohesion stresses in Fig. 8 for a gel made at rest and for gels made under two different stresses, 30 and 40 Pa. One can see a parallel evolution versus time for the cohesion stresses, indicating that an annealing process occurs for gels made under shear, by formation of new crosslinks between the polymer chains. The data has been taken at different moments, even after the cone rotation had stopped, and shows a continuous evolution. Comparing the results with those of Fig. 6a it is seen that elastic moduli G' tend to merge rapidly with the values measured at rest, while the cohesion stress increases parallel to the one of the gel made at rest, without reaching it, within the experimental time of observation. The gel keeps the memory of the particular way

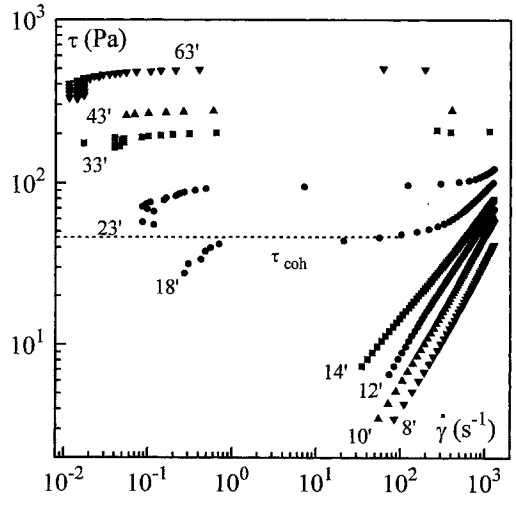

Fig. 7 Instant rheograms for gels prepared in quiescent conditions (c=6.5%, T=26 °C). The cohesion stresses τ_{coh} can be deduced from these plots

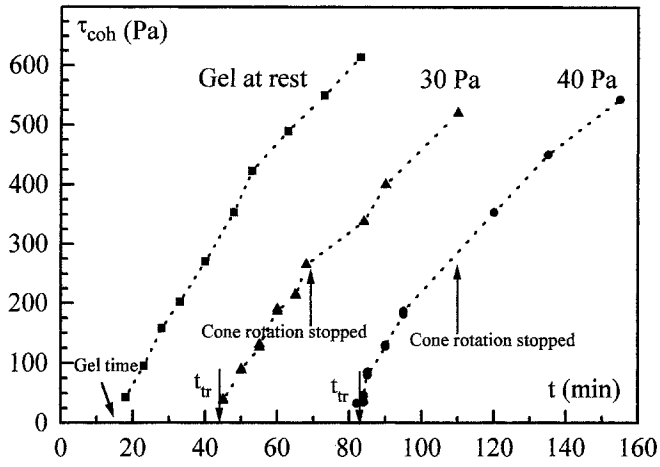

Fig. 8 Variation of the cohesion stresses versus time for gels made in quiescent conditions and for gels made under flow at constant shear stresses

it has been prepared: even if the linear properties are recovered, the non-linear behavior remains different for the cases investigated. The resistance against fracturing is weaker for gels made under shear.

The conclusions for gelation under constant shear stress are the following: a gelation transition occurs for gels made under shear at constant stresses. The gels may be called "particulate gels". Particulate gels can flow under shear and exhibit a yield stress and a cohesion stress. Gels made in quiescent conditions cannot flow and are characterized by their cohesion stresses, which probably correspond to their fracture. Soon after the gelation transition, the linear properties are recovered rapidly, however the non-linear properties are not recovered: gels keep the memory of the shearing effect and exhibit low cohesion stresses, a long time after the shear had stopped.

Gelation under controlled shear rates

A quite different behavior was observed for gels made under *a controlled shear rate*. The results are shown in Fig. 9a,b. The apparent viscosity is plotted versus time for the different imposed shear rates in Fig. 9a. Time is given in logarithmic scale up to 1000 min (15 h). The shear rate is controlled by the software of the instrument. The corresponding shear stresses versus time are given in Fig. 9b. The control of the shear rate by computer is difficult to achieve at the beginning of gelation, when the viscosity is low, in particular at low shear rates (3–10 s^{-1}) (Fig. 9b). Errors of 50% may appear by comparison to the reference shear rate. However, in this range (first 15 min) the viscosity is Newtonian and the shear rate has no effect upon the kinetics of gelation. During that time, gelation starts and viscosity increases

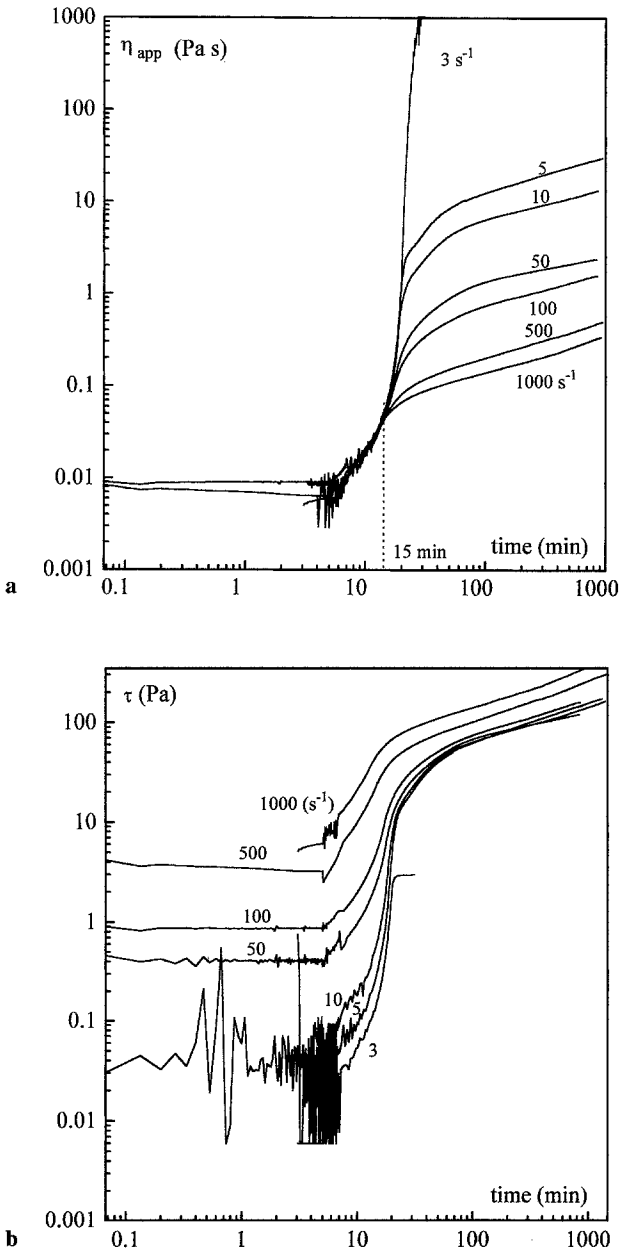

Fig. 9 Gelation for flows under controlled shear rates. The shear rates are indicated on the plots. **a** Apparent viscosities versus time in minutes, both in logarithmic scales. **b** shear stresses versus time in minutes in logarithmic scales. (c=6.5%, T=26 °C)

from 6 mPa s to 0.7 Pa s. At time $t > 15$ min, the effect of shear becomes visible. Also, the shear rate is better controlled, with an accuracy of a few percent. At low shear rate, a rapid gelation occurs, almost as in quiescent conditions (for instance $\dot{\gamma} \approx 3\ s^{-1}$). At intermediate values (5 to 50 s^{-1}) viscosity increases rapidly, up to few Pa s, then an abrupt change appears which we attribute to a fracturing of the fragile, just formed gel (data for 5 and 50 s^{-1} were obtained for almost the same

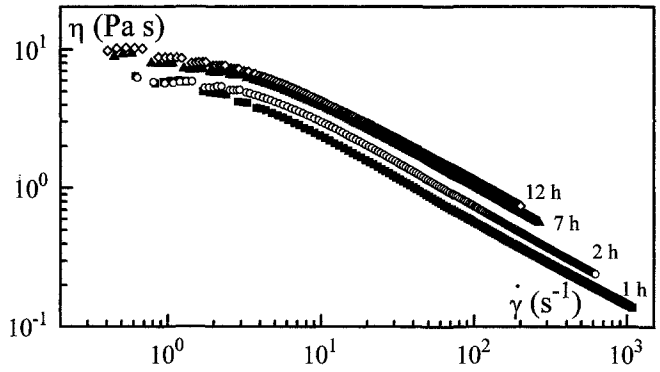

Fig. 10 Instant flow curves for solutions sheared under 100 s^{-1}. The rheograms are performed after 1, 2, 7, and 12 h

shear stresses (Fig. 9 b), thus we suspect that these data do not correspond to a homogeneous state of a fluid, but rather to a fracturing effect). The results are more clearly established for higher shear rates ($\dot{\gamma} > 50\ s^{-1}$). It is clearly seen in Fig. 9 a, that the viscosity remains finite after 15 h reaching values between 0.3 and 20 Pa s, the evolution proceeds rapidly at the beginning ($t < 40$ min) then is limited by the shear rate. Instant flow curves were performed to characterize the state of the solution after shearing, at shear rates $\dot{\gamma} > 50\ s^{-1}$.

The critical shear rate $\dot{\gamma}^*$ plays again the role of switching the process from a quick gelation to the maintain of the fluid state. Driving the rheometer in the shear rate-controlled mode is delicate when gelation starts.

Instant rheograms

When gelation proceeds under a shear rate $\dot{\gamma} > 50\ s^{-1}$, instant flow curves can be performed for increasing shear rates. Kinetics under different shear rates were analyzed, and showed comparable results. We report in Fig. 10 the viscosity versus shear rate in a double-logarithmic scale at different moments $t = 1$, 2, 7, 12 h for the gelation performed at 100 s^{-1}. The flow curves correspond to shear thinning fluids. Between 1 and 12 h the viscosity of the solutions show only minor changes. There is no indication for a gelation transition even after 12 h. A slow evolution of the viscosity is however observed.

Dynamic measurements: annealing effects

As the solutions under shear do not show gelation, we decided to investigate the process of annealing when the shear was stopped, for instance after 1 h shearing. The results are shown in Fig. 11 a, b and c, for G', G'' and the ratio G'/G'', for a gel made in quiescent conditions and for solutions which were let to gel after being sheared during 1 h, for three shear rates $\dot{\gamma} = 10$, 100 and 1000 s^{-1}. One can see that these solutions exhibit a $G' < G''$ as long as they are under shear (except may be for the one at $\dot{\gamma} = 10\ s^{-1}$ which shows a higher ratio, with, however, a G'' much larger than for the gel at rest). When one stops the shear, a rapid increase of G' and decrease of G'' is observed, showing the rapid gelation of the solutions. After 500 min, the solution sheared at a low shear rate had almost recovered the moduli of the quiescent gel, however a distinct shift persists for the solutions which were sheared at higher shear rates. The memory of the conditions is kept in these cases.

In conclusion, gelling solutions under constant shear rates, well above the critical shear rate, $\dot{\gamma}^*$, do not gel, only a moderate increase of the viscosity is observed. The solutions then are shear thinning fluids. When solutions are let in quiescent conditions after being sheared, they gel but the linear properties of the gels are not recovered and the gels distinctly keep the memory of the previous shearing. For shear rates slightly above $\dot{\gamma}^*$ we believe that we have a regime of fracturing of weak gels.

A qualitative picture of the effect of shearing on gelling solutions could be derived from the experimental data, but a theoretical interpretation of the flow curves helps to quantify these effects and to better understand their origin.

Theoretical background and interpretation

There is no theoretical model of gelation under shear. We have placed the theoretical interpretation in the framework of the models known for colloidal suspensions, rigid particles or flocculated suspensions, for particles which undergo Brownian movements. We first briefly recall these ideas.

It is known that suspensions exhibit shear thinning behavior, when the volume fraction of particles is high enough, > 20% for instance. The non-Newtonian behavior of colloidal suspensions has been modeled by Krieger and Dougherty (1959). The ideas put forward by Krieger and Dougherty deal with the description of the crowding effects due to the increasing volume fraction of particles. Increasing the volume fraction of particles favors the formation of transient doublets which behave like dumbbells when the shear rate is very low and which are dissociated by flow under high shear rates. The association/dissociation process is treated like a chemical reaction, where two species are present, singlets and doublets of particles. The kinetic equation governs the fraction of doublets in suspension. In the

Rheologica Acta, Vol. 36, No. 6 (1997)

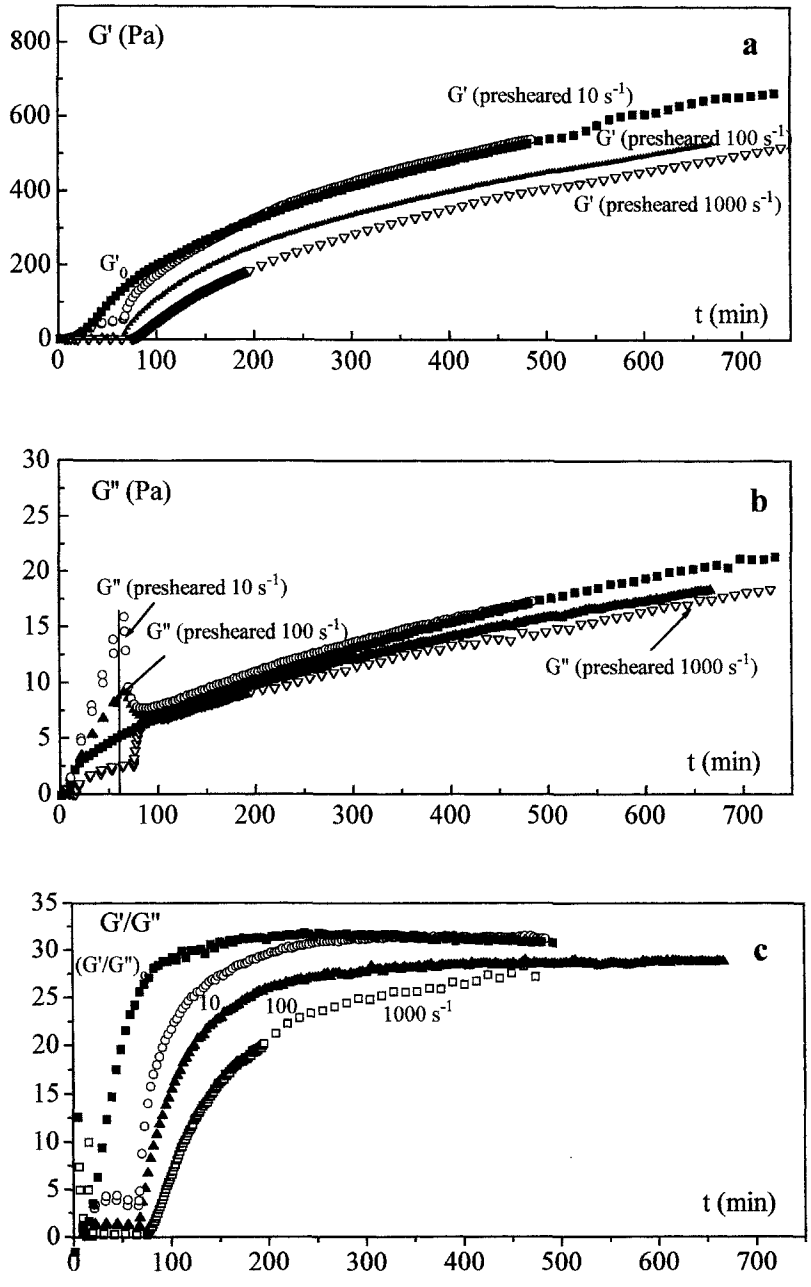

Fig. 11 Dynamic measurements for gels made in quiescent conditions and for solutions sheared during 1 h under 10, 100 and 1000 s^{-1} then let to gel at constant temperature. **a** G' versus time, **b** G'' versus time and **c** G'/G'' versus time

model of Krieger and Dougherty, the viscosity is related to the fraction of each species and varies with the shear stress τ: two limiting viscosities η_0 at low (zero) shear stress and η_∞ high (infinite) shear stress are introduced. The model has been extended to flocculated suspensions by Cross (1965, 1970), who derived, with slightly different assumptions, the equation which relates the viscosity η to the shear rate $\dot{\gamma}$, introducing also two limits, η_0 and η_∞, with a characteristic shear rate $\dot{\gamma}_c$. A power law dependence of the viscosity versus shear rate is expected, modulated by an exponent m, $0 < m < 1$. The Cross equation writes:

$$\frac{\eta - \eta_\infty}{\eta_0 - \eta_\infty} = \frac{1}{1 + (\dot{\gamma}/\dot{\gamma}_c)^m} \tag{2}$$

The slope of $\log \eta$ versus $\log \dot{\gamma}$ in the shear thinning region is related to m. The characteristic shear rate $\dot{\gamma}_c$ is located at $(\eta_0 + \eta_\infty)/2 \approx \eta_0/2$ if $\eta_\infty \ll \eta_0$. In the Cross model, the characteristic shear rate $\dot{\gamma}_c$ is expressed as a function of the kinetic constants of breaking links between particles, either spontaneously or by shear. For Brownian particles, a simple expression for $\dot{\gamma}_c$ can be alternatively derived by using a dimensionless parameter known in hydrodynamics as the Péclet num-

ber, Pe, which is the ratio of the Brownian diffusion time for a particle of radius R, at temperature T, diffusing in a suspending fluid of viscosity η_s and the time for convective movements in the shear flow, which is the inverse of the shear rate $\dot{\gamma}^{-1}$:

$$\mathrm{Pe} = \frac{\frac{6\pi\eta_s R^3}{kT}}{\dot{\gamma}^{-1}} \tag{3}$$

where k is the Boltzmann constant.

The characteristic shear rate $\dot{\gamma}_c$ corresponds to $\mathrm{Pe} = 1$ and thus writes:

$$\dot{\gamma}_c = \frac{kT}{6\pi\eta_s R^3} \tag{4}$$

The characteristic shear rate is directly related to the size of the particles.

In the phenomenological model due to Moore (see reference in Cheng, 1987), the non-Newtonian behavior of complex fluids is described with the help of a structural parameter λ. This model gives a more global view of the structure of shear thinning fluids, where the composition cannot be simply defined or is unknown. In the Moore model, the structural parameter varies between 0 and 1, depending on the shear rate. The viscosity is a linear function of the structural parameter. The structural parameter obeys a kinetic equation and for steady state measurements the equilibrium value λ_e is defined by:

$$\frac{\eta - \eta_\infty}{\eta_0 - \eta_\infty} = \lambda_e \tag{5}$$

and

$$\lambda_e = \frac{1}{1 + (\dot{\gamma}/\dot{\gamma}_c)^m} \tag{6}$$

In this model also the parameter $\dot{\gamma}_c$ is related to the kinetic constants of making and breaking the local structure. The equation derived by Moore is essentially the same as the Cross equation. More recent theoretical models known in the rheology of complex fluids are due to Quemada (1985) who introduced the concept of "structural units", whose effective volume fraction depends on the actual volume fraction of particles, Φ, and on the shear rate.

When yield stress fluids are investigated, shear thinning effects are observed when the applied stresses are larger than the yield stress. The gel-like structure of the suspension is then disrupted and the fluid is put under flow. The flow curves can be described by the equation similar to the one proposed by Worral and Tuliani (1964) which writes:

$$\tau = \tau_Y + \eta\dot{\gamma} \tag{7}$$

where η is given by the Cross Eq. (2).

Interpretation of the flow curves

The instant flow curves giving $\log\eta$ versus $\log\dot{\gamma}$ or $\log\tau$ versus $\log\dot{\gamma}$ show a strong time evolution, in particular the shift of shear rates for an almost identical range of stresses is visible. The shear thinning domain is progressively shifted towards low shear rates. We also identified, in Fig. 4a, the existence of a particular shear rate that we called the critical shear rate $\dot{\gamma}^*$. This brings us to the choice of the variable to analyze the flow curves, which thus appears to be the shear rate. The Cross equation will be used to analyze the flow curves during Stage I of the kinetics at constant shear stresses, and during the kinetics at constant shear rates.

The kinetics of gelation under shear can be described in the following way:

When gelatin is in the sol state, the viscosity is Newtonian for all the concentrations investigated and for the range of shear rates which is accessible. When the temperature is lowered to 26 °C, solutions start to gel, either at constant shear stress or shear rate. At the beginning, when the first clusters (microgels) are formed, the viscosity remains Newtonian. This suggests that the volume fraction of the clusters, which we assimilate to small particles, is not high enough to show crowding effects which are described by the Krieger and Dougherty model. The microgels have a certain internal cohesion, due to the helical crosslinking, which allows them to flow without being disrupted. Indeed, the flow curves can be almost superposed in sweeps of increasing, then decreasing shear stresses or shear rates, provided the range does not too greatly exceed the permamently applied values. For instance, the flow curves obtained for the kinetics under 40 Pa are reversible in the range 20 to 60 Pa. We shall take up this point later on.

Rheograms for the kinetics under constant shear stresses

The flow curves adjustment introduces four parameters: η_0, η_∞, $\dot{\gamma}_c$ and the exponent m. At the beginning, the ratio $\eta_0/\eta_\infty \approx 10$, then it increases with time to 2 or 3 decades. A good fit was obtained using the Cross equation, in the range of shear rates below the shear rate of the flow. According to the picture proposed by Krieger and Dougherty, the shear thinning effect is due to the decrease of the proportion of doublets versus singlets in the solution. For higher shear rates, however, a progressive disruption of the microgels occurs, leading to a continuous decrease of the viscosity. Thus, we privileged in the data fitting procedure the low shear rate part of the flow curves. For this reason, the precise measurement of η_∞ is not possible due to the fact that the microgels are torn and an important hysteresis arises

between the sweeps with increasing, then decreasing shear rates.

We focus now on the time evolution of the exponent m and of the characteristic shear rate $\dot{\gamma}_c$.

• Exponent m

The exponent m increases from a value close to 0.6 to nearly 1 when approaching the transition. This parameter has been related to polydispersity effects in the case of entangled polymer solutions, in particular an empirical relation has been found by Cross (1969) between the exponent m and the polydispersity index of the polymer solution. Shear thinning is expected in monodisperse polymer solutions and melts. Doi and Edwards (1979) established theoretically that the flow curves become unstable when the shear rate is much higher that the inverse of the characteristic time for polymer disentanglement, for narrow distribution melts of high molecular weight ("constitutive instabilities in shearing"). Another type of unstable flows was observed in micellar solutions by Makhloufi and Cressely (1992), corresponding to the formation of a nematic phase under shear (Cappelaere et al., 1994). The coexistence of the two phases in the gap of the rheometer induces a jump of the shear rate: the shear rate is not homogeneous and leads to emergence of layers having different viscosities. The large shear thinning effect that we observe in our case, just before the transition, may also indicate the presence of layers of different viscosities, but our way of interpreting the data favors the hypothesis of shearing of an homogeneous fluid. During the transition, the flow of the fluid shifts from a low viscosity state to a high viscosity state of the rheograms. Soon after the transition, a gel is formed (t=85 min) which has a yield stress.

In Stage II, flow curves were fitted using Eq. (7). Again, we found the exponent $m=1$ for the viscosity of the fluid η above the yield stress. The curves $\log \tau$ versus $\log \dot{\gamma}$ are even more markedly flat in the region of the cohesion stress. As soon as the cohesion stress is reached (Fig. 5b), the shear rate increases rapidly: the rheograms show a strong thixotropy, by decreasing the stress, we observe very large hysteresis loops, indicating that there was an important disruption of the aggregated structure. When the shear stress on the flow curves remains < 100 Pa (gelation under 40 Pa) the flow is almost reversible: this corresponds to the condition that the shear rate remains below $\dot{\gamma}^*$.

• The characteristic shear rate $\dot{\gamma}_c$

The most striking feature that appeared for gelation under constant shear stress is the time evolution of the characteristic shear rate $\dot{\gamma}_c$. In Fig. 12, we plot the time evolution of the shear rate $\dot{\gamma}$ and of the characteristic shear rate $\dot{\gamma}_c$ during the flow under $\tau=40$ Pa. The transition time t_{tr} is indicated in the plot. In Stage I, the solution flows with a shear rate $\dot{\gamma}$ which is approximately $\dot{\gamma} \approx 10\ \dot{\gamma}_c$, with a Péclet number Pe=10. This number is the same for the three kinetics investigated in detail, at $\tau=30$, 40 and 60 Pa.

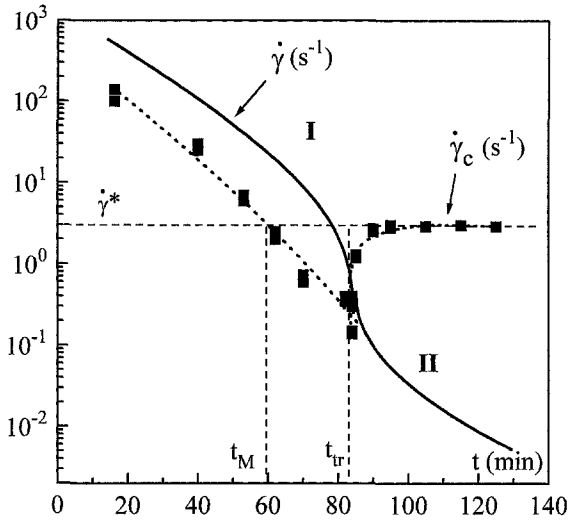

Fig. 12 Time dependence of the shear rate $\dot{\gamma}$ and of the characteristic shear rate $\dot{\gamma}_c$ for gelation under constant shear stress of 40 Pa

When the transition time is approached, the shear rate is close to $\dot{\gamma}^*=3\ s^{-1}$. At the transition time t_{tr}, the shear rate of the flow decreases rapidly, while the characteristic shear rate $\dot{\gamma}_c$ of the rheograms varies in the opposite way and increases rapidly. In Stage II, the shear rate of the flow still decreases, until the cone rotation is stopped. Shortly after the transition, we observe on the rheograms that $\dot{\gamma}_c = \dot{\gamma}^* = 3\ s^{-1}$ and $\dot{\gamma} \leq 0.1\ \dot{\gamma}_c$; the ratio $\dot{\gamma}/\dot{\gamma}_c$ decreases strongly with time.

We have noticed that the particular shear rate $\dot{\gamma}^*$ plays the role of a switch parameter for the kinetics of gelation. Thus, when the characteristic shear rate $\dot{\gamma}_c$ decreased below $\dot{\gamma}^*$, in Stage I, we expected to observe gelation shortly after. We call t_M the moment when $\dot{\gamma}_c$ becomes $\dot{\gamma}_c < \dot{\gamma}^*$. In the range of times $t_M < t < t_{tr}$, the state reached by the fluid can be described as a "metastable state". This means that as long as the solutions are flowing at a shear rate higher than $\dot{\gamma}^*$, the fluid state is maintained, but at any moment when the fluid is brought at shear rates below $\dot{\gamma}^*$, it tends to gel very quickly. In this particular range, the flow curves show instability (exponent $m \approx 1$). We can summarize the evolution of the fluid under a fixed shear stress according to the shear rate of the continuous flow in three steps:

- for $t < t_M$, the shear rate of the continuous flow is $\dot{\gamma} > \dot{\gamma}_c > \dot{\gamma}^*$, one has a stable fluid state
- for $t_M < t < t_{tr}$, the shear rate of the continuous flow is $\dot{\gamma} > \dot{\gamma}^* > \dot{\gamma}_c$, one has a metastable fluid state

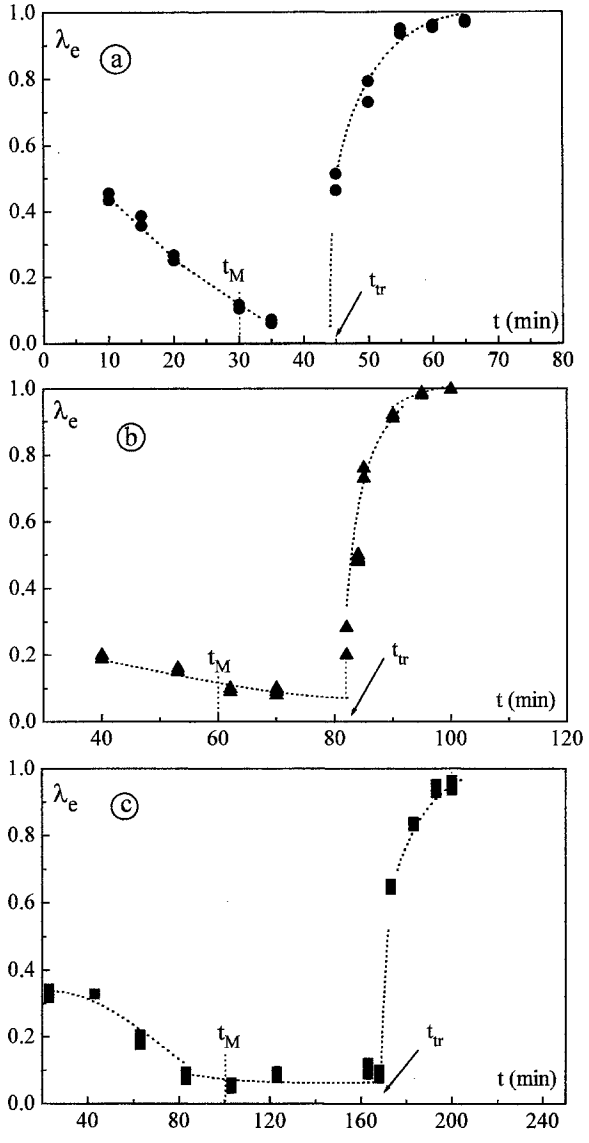

Fig. 13 Changes of the structural parameter λ_e during gelation at constant shear stresses. The results for three kinetics under constant shear stresses are given: (**a**) 30, (**b**) 40 and (**c**) 60 Pa

– $t > t_{tr}$, the shear rate of the continuous flow is $\dot{\gamma} < \dot{\gamma}_c = \dot{\gamma}^*$, one has a yield stress fluid under flow.

• Parameter λ_e

Following the definition of the structural parameter due to Moore, we have calculated λ_e at different moments of the process using Eq. (6). The results are given in Fig. 13 for three kinetics: 30, 40 and 60 Pa. In Stage I, $t < t_M$, $\lambda_e \approx 0.2$ to 0.4 and reaches very low values $\lambda_e = 0.1$ in the metastable region, $t_M < t < t_{tr}$. After the transition, in Stage II, the structural parameter λ_e increases rapidly and reaches a value close to 1, $\lambda_e \approx 1$. The fluid which is now a yield stress fluid flows at a shear rate which allows a maximum of structure to be present during flow. The abrupt increase of λ_e from 0.1 to 1 at the transition is reminiscent of the step-like evolution of the order parameter in first order thermodynamic phase transitions: the disordered phase would be Stage I (fluid state), the ordered phase would be the yield stress "fluid gel" (Stage II). The parameter which controls the transition is the volume fraction of microgels (see below) which increases with time.

Rheograms for the kinetics under constant shear rates

The Cross equation has been used to fit the flow curves obtained in gelation under a fixed shear rate. In this case no yield stress fluid appeared. For the kinetics under 100 and 500 s^{-1}, after 2 or 3 h shearing, the instant rheograms clearly show an exponent $m=0.74$ and $\dot{\gamma}_c \approx 10$ to 20 s^{-1}. The solutions did not reach the metastable state, when $\dot{\gamma}_c < \dot{\gamma}^*$ and $m \approx 1$.

Structural model

It is possible to further interpret the evolution of the structure of the gelling solutions by examining the Péclet numbers. As stated at the beginning, the Péclet number for a colloidal suspension is related to the size of the particles. The characteristic shear rate $\dot{\gamma}_c$ of a suspension is directly related to the size of the particles through Eq. (4). We used this equation in order to derive the radius R of the microgels. For this we needed to introduce a local viscosity η_s of the surrounding fluid. We have chosen the viscosity of the sol state, where the molecules are in the coil state. For instance, $\eta_s = 6.5$ mPa s for the gelatin solution of concentration 6.5%. We shall discuss this point later. This allows us to plot in Fig. 14a and b the time evolution of the radii of the microgels, during gelation under fixed shear stresses or fixed shear rates. It is seen in Fig. 14a that the radii of the microgel particles increase with time in Stage I, from a minimum value of the order of $R_{min}=100$ nm to a maximum $R_{max}=500$ nm at the transition. Similar values appear in the three kinetics. In Stage II we also used the Péclet number to calculate the radii of the microgels which now are assembled, at rest, in a network. If we keep the same definition, we can see that the radii of individual particles which can be found in the sheared gels are now smaller by a factor of 2, as compared to their size just before the transition and reach a limit that we call $R^*=220$ nm. This value may be understood as the "hard core" of the microgel particles. The dissociation of the microgels R_{max} into microgels of size R^* occurs under the stress τ_{coh}. The cohesion stress increases with time: as the gel modulus,

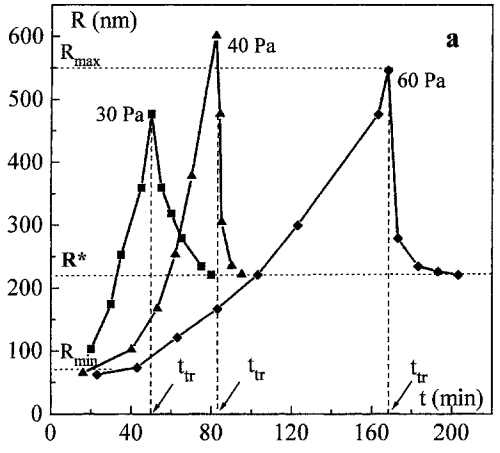

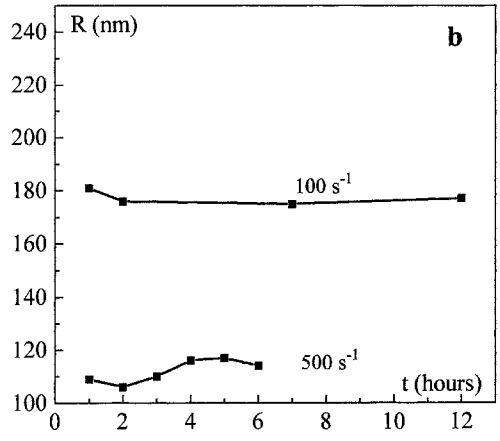

Fig. 14 Increase of the size of microgel particles versus time, derived from the Péclet number Pe.
a Gelation under stresses of 30, 40, 60 Pa. The microgel radii increase in Stage I, until they reach a maximum value, $R_{max}=500$ nm when percolation occurs. In Stage II the size of this elementary microgel $R^*=220$ nm corresponds to the scission of the microgel R_{max} when the shear stress reaches the coherence stress τ_{coh}. R^* is considered as a hard core of the microgels.
b For gelation under fixed shear rates of 100 and 500 s^{-1}, the size of the microgels remains constant after 1 h

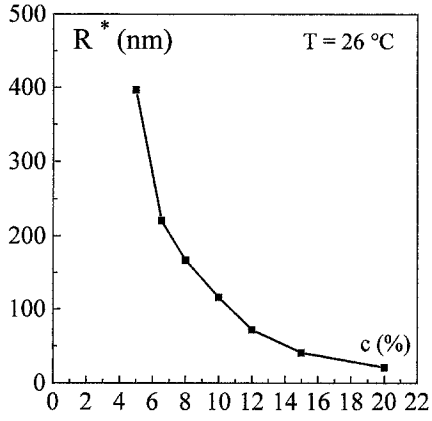

Fig. 15 Size R^* as a function of the gelatin concentration for gelation at $T=26$ °C

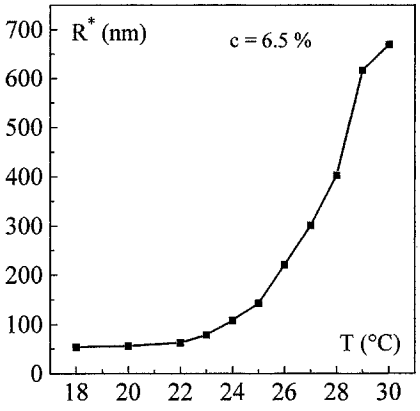

Fig. 16 Size R^* as a function of the gelation temperature for a fixed concentration of 6.5%

G', the internal elastic moduli of the particles increase, and higher stresses are needed to disrupt them.

For gelation under fixed shear rates, 100 and 500 s^{-1} (Fig. 14b) the radii of microgels remain constant and are below R_{max}.

We also investigated the effect of the gelatin concentration and of the gelation temperature, for gelation under constant shear stresses. The critical shear rate $\dot{\gamma}^*$, determined from the continuous flow curves, varies significantly. If we keep the idea that, in Stage II, the characteristic shear rates $\dot{\gamma}_c \approx \dot{\gamma}^*$, then we can derive the different "hard core" sizes, R^*. The values for $R^*(c)$ for a gelation temperature of $T=26$ °C, are shown in Fig. 15 and $R^*(T)$, T being the gelation temperature, for a concentration of 6.5%, in Fig. 16. The lowest temperatures and the largest concentrations correspond to the smallest values of R^*. A saturation effect is seen in these limits but, over the whole range, large variations distinctly appear.

All these observations can be included in a global picture of gelation under shear. The scheme, we arrived at, is the following:

in the sol state, the gelatin solution is Newtonian. When the solution is cooled triple helical sequences start to nucleate at random along the chains and create junctions between them. It is known for these gels that the lower the temperature and the higher the concentration, the more important the number of nucleated helical sequences. Clusters of chains are thus formed from the very beginning, as soon as the temperature is lowered, but their volume fraction is low and the solutions behave as Newtonian fluids. After this period, the imposed stresses or shear rates modify the kinetics of gelation, and at the same time, the instant rheograms

show shear thinning. The solution then behaves like a suspension of clusters or microgels surrounded by the solution of entangled coils, which constitutes a reservoir for the growth of the microgels: when new helices are formed, they attach other coils to the existing microgels, which then grow in size. The volume fraction of microgels increases versus time. According to the Krieger and Dougherty model, the instant rheograms may reveal the flow of doublets, at low shear rates, and singlets at high shear rates. As the microgels are surrounded by the solution in the coil state, we assumed that the local viscosity of the solutions is that of the sol state. When a critical volume fraction is reached, percolation between microgels occurs which induces the sol-gel transition. We noticed that R_{max} is the same for the different applied stresses, the shear rate at which the solutions flow at that moment was also the same ($\dot{\gamma}^*$). So, we conclude that the critical volume fraction of microgels is independent of the shear stress. This means that the number of clusters per unit volume is independent of the history of the solution; this number is fixed from the beginning of the gelation when, indeed, the shear has no effect on the kinetics. Only temperature and concentration have an influence on the number of initial clusters, which is thus related to the nucleation process at the beginning of gelation. In Stage II, the microgels can link to each other by new crosslinks (the yield stress increases), however, when the gel is submitted to shear, some weak links are broken, the gel can flow. By analogy with Stage I, we associate to the characteristic shear rate $\dot{\gamma}_c = \dot{\gamma}^*$ a size R^*. This size can be interpreted as a "hard core" of the microgels. Flow beyond the shear rate $\dot{\gamma}^*$ dissociates the clusters R_{max} into units, R^*, when the cohesion stress τ_{coh} is applied. The flow during the breaking is unstable and a large hysteresis in the shear rate sweeps appears, when the gels are sheared.

The last point to comment on should be the metastability of the solution after the time t_M. We suggest that, at this moment, the volume fraction is sufficiently high for percolation to occur at low shear rates (solutions gel very quickly when the shear rate is lowered), but it is below the volume fraction needed for percolation of the clusters under flow. Indeed, in suspensions of hard spheres, it has been established (Quemada, 1985) that the maximum volume fraction, at which a fluid gels (maximum packing), depends on the shear rate and this has been explained by the concept of "effective volume fraction": the effective volume fraction depends on the shear rate and the maximum increases with the shear rate. The volume fraction of the microgels at the gel point may be very low compared to the hard spheres packing, due to the polymeric nature of the network, nevertheless an analogy can be suggested between these two situations. Another interesting point appearing in this study is the proof that a gelatin gel can exhibit

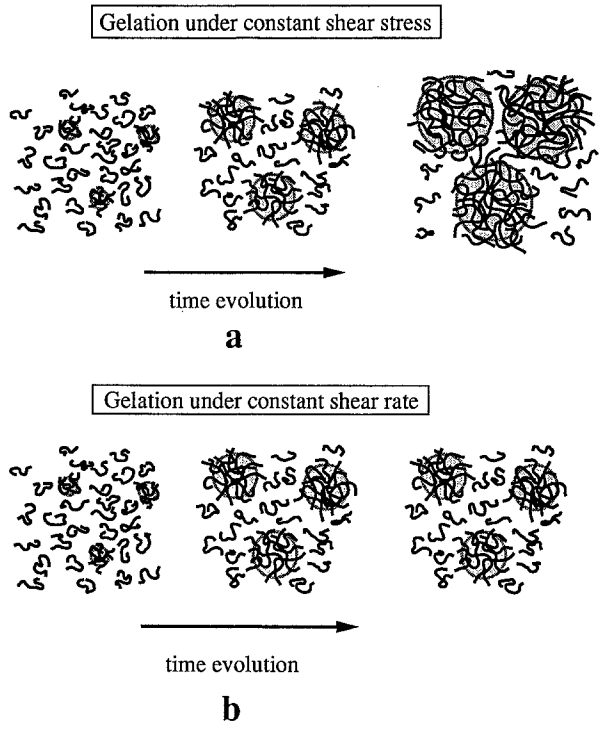

Fig. 17 Schematic representation of the time evolution of the microgels: **a** for gelation under constant shear stress and **b** under constant shear rate, above the critical shear rate

healing effects, microgels being able to crosslink each other. A broken gelatin gel, made under quiescent conditions, is not able to heal. We believe that this is due to the fact that a reservoir of chains in the coil conformation surrounds the microgels and is free to participate in new junctions.

For solutions sheared at constant shear rates, above 50 s^{-1}, the volume of microgels does not reach the critical volume fraction necessary for the percolation of the clusters (the clusters are still too small after 12 h). A slow progressive increase of the apparent viscosity over a long period of time is, however, observed which may be attributed to possible nucleation of new clusters, their maximum size being limited by the shear rate.

The whole process of gelation under shear is summarized schematically in Fig. 17.

Conclusion

The aim of this study was to determine the evolution of a solution where gelling and shearing operate simultaneously and in opposite ways. We have imagined a process of gelation which takes place under a fixed shear stress or a fixed shear rate. We found basically two regimes, one which allows gelation under shear and another which impedes gelation. A critical shear rate

clearly plays the role of a switch for the evolution of the solution. The gelatin gel recovers its linear properties after some time at rest, but remains more fragile under large stresses. In order to elucidate the microscopic aspects involved in this investigation, an experimental device is being built in our laboratory combining ellipsometric techniques and rheology, which allows to measure simultaneously the optical rotation (amount of helices present) and the birefringence (due to orientation effects) in the solutions gelling under shear.

This study suggests new routes for processing solutions which undergo gelation, polymerization and phase separations.

Acknowledgements This study was supported by Société Nationale Elf Aquitaine and was part of the research project TIFAN associating CNRS and INRA. The authors are grateful to M. Bourrel, D. Quemada, J.F. Lequeux, H. Herrmann for many interesting discussions. The gelatin sample was kindly provided by Société SBI. The authors wish to thank G. Takerkart and A. Denis for their help and advice.

References

Berret JF, Roux DC, Porte G (1994) Isotropic to nematic transition in wormlike micelles under shear. J Phys II France 4:1261

Beysens D, Gbadamassi M, Moncef-Bouanz B (1983) New developments in the study of binary fluids under shear flow. Phys Rev A 28:2491

Bourgoin D, Joly M (1952) La transformation sol-gel de la gélatine. Étude par la biréfringence d'écoulement. J Chim Phys 49:427; (1954) Nouvelles recherches sur les mécanismes de gélification. I Résultats expérimentaux, Kolloid Z 136:25; (1956) Nouvelles recherches sur les mécanismes de gélification. II Interprétation des résultats expérimentaux. Kolloid-Z 146:121; (1958) Nouvelles recherches sur les mécanismes de gélification. III Phénomènes de prégélification dans les solutions da gélatine. Verh Kolloid Ges 18:36

Cappelaere E, Cressely R, Makhloufi R, Decruppe JP (1994) Temperature and flow induced viscosity transition for CTAB surfactant solutions. Rheol Acta 33:431

Chan CK, Perrot F, Beysens D (1991) Experimental study and model simulation of spinodal decomposition in a binary mixture under shear. Phys Rev A 43:1826

Cheng DC-H (1987) Thixotropy. Internat J of Cosmetic Sci 9:151

Cross MM (1965) Rheology of non-Newtonian fluids: a new flow equation for pseudo-plastic systems. J Colloid Sci 20:417; (1970) Kinetic interpretation of non-Newtonian flow. J Colloid & Interface Sci 33:30

De Carvalho W, Djabourov M (1994) Prise en gel des solutions de gélatine sous cisaillement. Les Cahiers de Rhéologie 13:247; (1995) Agrégation et rhéofluidification: effect des contraintes et des gradients de cisaillement sur un gel physique. ibid 14:637

de Gennes PG (1976) On the relation between percolation theory and the elasticity of gels. J Phys Lett 37:L 1

Decruppe JP, Cressely R, Makhloufi R, Cappelaere E (1994) Flow birefringence experiments showing a shear banding structure in a CTAB solution. Colloids Polym Sci 273:346

Diat O, Roux D, Nallet F (1993) Effect of shear on a lyotropic lamellar phase. J Phys II France 3:1427

Djabourov M, Leblond J, Papon P (1988a) Gelation of aqueous gelatin solutions. I. Structural investigation. J Phys France 49:319; (1988b) Gelation of aqueous gelatin solutions. II. Rheology of the sol-gel transition. Ibid 49:333

Doi M, Chen J (1989) Simulation of aggregating colloids in shear flow. J Chem Phys 90:5271

Doi M, Edwards SF (1979) Dynamics of concentrated polymer systems. IV. Rheological properties. JCS Farad Trans 2, 75:38

Hashimoto T, Takebe T, Suehiro S (1988) Ordered structure and critical phenomena of semidilute solutions of polymer mixtures under shear flow. J Chem Phys 88:5874

Hobbie EK, Hair DW, Nakatani AI, Han CC (1992) Crossover to strong shear in a low molecular weight critical polymer blend. Phys Rev Lett 69:1951

Horst R, Wolf BA (1993) Refined calculation of the phase separation behaviour of sheared polymer blends: closed miscibility gaps within two ranges of shear rates. Macromol 26:5676

Joly M (1951) Orientation par écoulement de particules rigides qui se repoussent. Application à la biréfringence dynamique. Le Journal de Physique et le Radium 12:900; (1952) The use of streaming birefringence data to determine the size and distribution of rod shaped interacting particles. Trans Farad Soc 48:279; (1958a) Molecular association induced by flow in solutions of some macromolecular polyelectrolytes. Disc Farad Soc 25:150; (1958b) Changements de structure provoqués par l'écoulement. Rheol Acta 1:180; (1962) Le rhéoturbidimétrie: une nouvelle méthode d'étude des solutions colloïdales. Kolloid-Z 182:133

Joly M, Barbu E (1949) Étude par la biréfringence d'écoulement de la dénaturation thermique de la sérumalbumine. Bull Sté Chim Biol 31:1642; (1950a) Mécanisme de gélification de la sérumalbumine: étude par biréfringence d'écoulement. Ibid 32:116; (1950b) Biréfringence d'écoulement des solutions alcalines de sérumalbumine de cheval: étude du mécanisme de l'hydrolyse. ibid 32:123; (1950c) Action des électrolytes sur l'agrégation de la sérumalbumine: étude par la biréfringence d'écoulement. ibid 32:908; (1951) Étude par la biréfringence d'écoulement de l'agrégation thermique de la sérumalbumine. J Chim Phys 48:636

Krieger IM; Dougherty TJ (1959) A mechanism of non-Newtonian flow in suspensions of rigid spheres. Trans Soc Rheol III: 137

Larson RG (1992) Flow induced mixing, demixing and phase transitions in polymeric liquids. Rheol Acta 31:497

Makhloufi R, Cressely R (1992) Temperature dependence of non-Newtonian viscosity of elongated micellar solutions. Colloid and Polym Sci 270:1035

Mason TG, Bibette J (1996) Emulsification in viscoelastic media. Phys Rev Lett 77:3481

Min KY, Goldburg WI (1993) Nucleation of a binary liquid mixture under shear flow. Phys Rev Lett 70:469

Nakatani AI, Kim H, Takahashi Y, Matsushita Y, Takano A, Bauer BJ, Han CC (1990) Shear stabilization of critical fluctutations in bulk polymer blends studied by small angle neutron scattering. J Chem Phys 93:795

Onuki A, Kawasaki K (1979) Nonequilibrium steady state of critical fluids under shear flow: a renormalization group theory. Ann Phys NY 121:456

Quemada D (1985a) Relation comportement-structure dans les dispersions concentrées. Revue Générale de Thermique Fr 279:174; (1985b) Phenomenological rheology of concentrated dispersions. I. Clustering effects and structure dependent packing fraction. J Mecan Theor Appl, Numero Special: 267; (1985c) Phenomenological rheology of concentrated dispersions. II. Shear viscosity discontinuities as structure transitions. ibid:289

Rangel-Nafaile C, Metzner AB, Wissbrun KF (1984) Analysis of stress induced phase separations in polymer solutions. Macromol 17:1187

Stauffer D (1976) Gelation in concentrated critically branched polymer solutions. JCS Farad Trans II 72:1354

te Nijenhuis K (1997) Thermoreversible networks. Adv Polym Science 130

Worral WE, Tuliani S (1964) Viscosity changes during the ageing of clay-water suspensions. Trans Br Ceram Soc 63:167

West AHL, Melrose JR, Ball RC (1994) Computer simulations of breakup of colloid aggregates. Phys Rev E 49:4237

Wolf BA (1984) Thermodynamic theory of flowing polymer solutions and its application to phase separation. Macromol 17:615